

---

# POINTMANIFOLD CUT: POINT-WISE AUGMENTATION IN THE MANIFOLD FOR POINT CLOUDS

---

**Tianfang Zhu**

Britton Chance Center for Biomedical Photonics  
Huazhong University of Science and Technology  
Wuhan, Hubei 430074  
ztfun@hust.edu.cn

**Yue Guan**

Britton Chance Center for Biomedical Photonics  
Huazhong University of Science and Technology  
Wuhan, Hubei 430074  
yguan@hust.edu.cn

**Anan Li**

Britton Chance Center for Biomedical Photonics  
Huazhong University of Science and Technology  
Wuhan, Hubei 430074  
aali@hust.edu.cn

September 16, 2021

## ABSTRACT

Augmentation can benefit point cloud learning due to the limited availability of large-scale public datasets. This paper proposes a mix-up augmentation approach, PointManifoldCut, which replaces the neural network embedded points, rather than the Euclidean space coordinates. This approach takes the advantage that points at the higher levels of the neural network are already trained to embed its neighbors relations and mixing these representation will not mingle the relation between itself and its label. This allows to regularize the parameter space as the other augmentation methods but without worrying about the proper label of the replaced points. The experiments show that our proposed approach provides a competitive performance on point cloud classification and segmentation when it is combined with the cutting-edge vanilla point cloud networks. The result shows a consistent performance boosting compared to other state-of-the-art point cloud augmentation method, such as PointMixup and PointCutMix. The code of this paper is available at: <https://github.com/fun0515/PointManifoldCut>.

## 1 Introduction

Rapidly developing 3D reconstruction technologies such as LiDAR scanners and other sensors [1] can directly generate massive point clouds, which are widely used in fields, including autonomous driving [2], geographical mapping [3] and so on. To meet the needs of these applications, a series of data-driven approaches for learning features from point clouds have been proposed in recent years [4, 5]. These methods can be used for several visual tasks, such as point cloud classification [6–9], point cloud segmentation [10–12] as well as point cloud generation [13, 14]. However, over-fitting and poor generalization [5] caused by the dwarf scale of the existing public point cloud datasets [15, 16] is one of the challenges faced by many point cloud processing and analysis methods.

Inspired by the mixed sample data augmentation in image domain [17–19], researchers have been exploring augmen-

tation methods to create new training data from existing point clouds in recent years. PointMixup [20] defines a data augmentation between the point clouds as a shortest path linear interpolation, which solves the problem of point mismatch, and can be applied to the object-level point cloud classification. PointCutMix [21] directly replaces the point sets in two point clouds to obtain new training data. Since no new points are generated in this process, it can also be used for point cloud segmentation in addition to object-level classification. However, the change of neighborhood may cause the distortion of point-wise label and hinder the improvement on the network performance, due to the semantic information of points not only comes from themselves, but also from their neighborhood in the point cloud.

In this paper, we note that many learning-based point cloud processing methods constantly update the features of each point from the neighbor nodes [8,9], so the node features in

a high-dimensional manifold contain the knowledge about itself and its neighborhood, which are more compatible with the semantic labels than the original Euclidean spatial coordinates. From this observation, this paper proposes a point-wise data augmentation method, named PointManifoldCut, which replaces the points with the corresponding labels from different samples on manifold to generate new training data. This technique is verified in point cloud classification and segmentation tasks respectively, and it achieves the cutting-edge results in both tasks, which can consistently improve the performance of various vanilla networks by about 0.4% to 2.3%. We also show that this data augmentation method is insensitive to the point selection and is expected to be applied to a broader range of point cloud learning tasks.

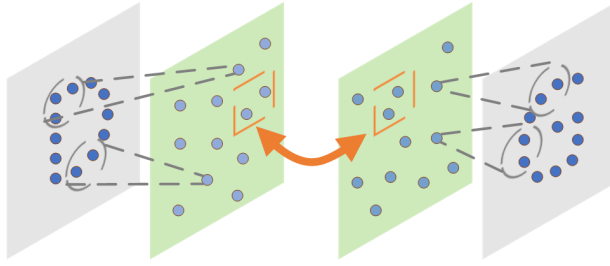


Figure 1: **PointManifoldCut: replace points in the manifold.** The dark and light blue represent the point clouds in Euclidean space and their corresponding manifolds in the embedded space respectively. Each point in the manifold contains the information about itself and its neighborhood.

## 2 PointManifoldCut

### 2.1 Problem statement

Here we focus on two basic point cloud processing tasks: point cloud classification and point cloud segmentation, while the latter can be regarded as point-wise classification. A training set containing  $J$  point clouds is given as  $\{(P_j, c_j, S_j)\}_{j=1}^J$ , where  $P_j = \{p_n^j\}_{n=1}^N \in P$  is a point cloud sample consisting of  $N$  points. Usually the initial feature of the point is the 3D coordinates of Euclidean space, as  $p_n^j \in \mathbb{R}^3$ .  $c_j \in \{0, 1\}^{C_1}$  is the one-hot class label for a total of  $C_1$  classes of each point cloud, while  $S_j = \{s_n^j\}_{n=1}^N$ , where  $s_n^j \in \{0, 1\}^{C_2}$ , is the one-hot class label for a total of  $C_2$  classes of each point in each point cloud.

A standard point cloud classification task aims to train a function  $h_c: P \rightarrow [0, 1]^{C_1}$  that maps a point cloud to a object-level semantic label distribution. So the function  $h_c$  can be learned by minimizing the loss as

$$\theta^* = \operatorname{argmin}_{\theta} \sum_{p \in P} L(h_c(p), c) \quad (1)$$

where  $\theta$  is the trainable parameter and  $L$  denotes the loss function such as the cross-entropy loss function. Likewise, the goal of a typical point cloud segmentation task is to learn a function  $h_s: (p, c) \rightarrow [0, 1]_N^{C_2}$  that maps a point cloud to a point-wise semantic label distribution, which

can be described as

$$\theta^* = \operatorname{argmin}_{\theta} \sum_{p \in P} L(h_s(p, c), s^N) \quad (2)$$

, where  $h_c(p)$  and  $h_s(p, c)$  respectively represent the output of classification networks and segmentation networks.

### 2.2 Algorithm

The purpose of PointManifoldCut is to create new training sample  $(g_k(\tilde{p}), \tilde{c}, \tilde{s})$  through the substitution of points in manifold domain from two available samples, where  $g_k$  is the mapping from the input data to the hidden representation at layer  $k$ . So the deep network  $h$  in (1) and (2) can be denoted as  $h(p) = h_k(g_k(p))$ . Here,  $h_k$  illustrates the mapping from the hidden representation layer  $k$  to the output, while  $p, c$  and  $s$  are the training point cloud, corresponding object-level and point-wise label, respectively.

The PointManifoldCut operation,  $PMC(b, b', M)$ , for batch  $b$ , shuffled batch  $b'$ , and mask  $M$  at layer  $k$  can be defined for two available training samples  $(p_1, c_1, s_1)$  and  $(p_2, c_2, s_2)$  without loss of generality:

$$\begin{aligned} g_k(\tilde{p}) &= M \cdot g_k(p_1) + (I_N - M) \cdot g_k(p_2) \\ \tilde{c} &= \lambda c_1 + (1 - \lambda) c_2 \\ \tilde{s} &= M \cdot s_1 + (I_N - M) \cdot s_2 \end{aligned} \quad (3)$$

, where  $M = \operatorname{diag}\{m_1, m_2, \dots, m_N\}$  and  $m_i$  is a boolean element indicating whether the  $i^{\text{th}}$  point is selected, which can be regarded as the Mask Scheme in image domain.  $I_N$  is an identity matrix with  $N$  diagonal elements.  $\lambda \in [0, 1]$  and it follows the  $\text{Beta}(\beta, \beta)$  distribution, indicating the ratio of selected points from the two training samples.

Furthermore, hyperparameter  $\rho \in [0, 1]$  is introduced to precisely control the chances that PointManifoldCut will be used. When  $\rho = 0$ , point clouds will not be augmented. Otherwise PointManifoldCut will be used for all the point clouds when  $\rho = 1$ . Hence the two kinds of loss function can be mathematically denoted as:

$$\begin{aligned} L_c(h) &= \sum_{p \in P} (1 - \rho) L(h(p), c) + \rho L(h(\tilde{p}), \tilde{c}) \\ L_s(h) &= \sum_{p \in P} (1 - \rho) L(h(p, c), s) + \rho L_s(h(\tilde{p}, \tilde{c}), \tilde{s}) \end{aligned} \quad (4)$$

where  $L_c$  and  $L_s$  respectively represent the loss function of point cloud classification and segmentation task. Algorithm 1 shows the general process of PointManifoldCut during training, where the  $\text{Uniform}(0, 1)$  represents generate a random number that follows the Uniform distribution and  $\operatorname{diag}(a, b)$  represents a diagonal matrix where the first  $a$  elements are 1 and the remaining  $b$  elements on the diagonal are 0.  $1(M)$  is the function to find how many element 1 are there in matrix  $M$ .

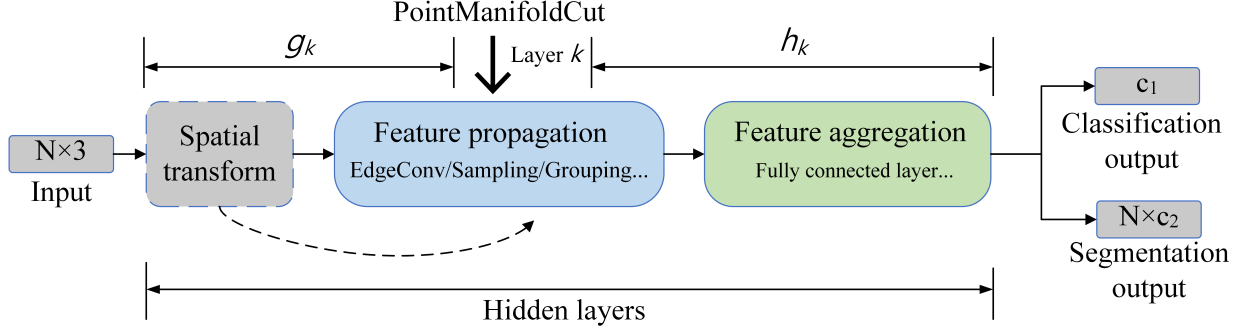


Figure 2: **A typical point cloud neural network for point cloud classification and semantic segmentation.** It can be divided into the propagation stage, where shape features are captured, and the aggregation stage that decodes features into the output score vectors. Some network example components are presented in the figure, such as EdgeConv in DGCNN and sampling layers in PointNet++. Spatial transformation is a frequently employed operator to align point clouds in the Euclidean space. We recommend using PointManifoldCut in the propagation phase and moving spatial transform after the PointManifoldCut to align the new samples.

---

**Algorithm 1** PointManifoldCut(PMC)

---

**Input:** Deep networks  $h$ , training batch  $b : (i, t)$  where  $i$  and  $t$  are the input and target of  $h$ .

**Parameter:** Threshold  $\rho \in [0, 1]$ ,  $\beta > 0$  and the number of points  $n$ .

**Output:** Value  $l$  of criterion  $L$ .

**Process:**

```

1:  $\theta = \text{Uniform}(0, 1)$ 
2: if  $\theta < \rho$  then
3:    $\lambda = \text{Beta}(\beta, \beta)$ 
4:   Initialize  $M \leftarrow \text{diag}(\lfloor \lambda \times n \rfloor, \lfloor (1 - \lambda) \times n \rfloor)$ 
5:   New batch  $\tilde{b} : (\tilde{i}, \tilde{t}) \leftarrow \text{PMC}(b, \text{shuffle}(b), M)$ 
6:   Update  $\lambda \leftarrow 1(M)/n$ 
7:    $l \leftarrow L(h(\tilde{i}), \tilde{t})) \times \lambda + L(h(\tilde{i}), t) \times (1 - \lambda)$ 
8: else
9:    $l \leftarrow L(h(i), t)$ 
10: end if
11: return  $l$ 

```

---

### 2.3 Analysis

In this section, we analyze some factors that may significantly affect the performance of PointManifoldCut, including the location where PointManifoldCut is used, the strategy of replacement points, as well as the impact of spatial transform.

**How to choose the layer  $k$ .** Although PointManifoldCut can be used after any hidden layer of point cloud processing networks, we recommend using it in the propagation stage of features to capture and utilize the shape features of the new samples. Fig. 2 shows the overall architecture of the vanilla networks for two point cloud tasks. These models are generally divided into three stages: the spatial transform for aligning point clouds, the feature propagation for learning local shapes, and the feature aggregation that aims to decoding features into output vectors. In contrast, the propagation phase is generally similar, while the aggregation phase will have different structures according

to different tasks. Therefore, setting PointManifoldCut operation in the feature propagation stage can reduce the changes to the network architecture. And according to this structure, PointCutMix [21] can be regarded as a special case of our methods at the input layer.

**Does the replacement method of points matter?** There are two different replacement methods for point clouds. One is to randomly select a series of points for replacement, the other is to randomly select a central point in the second cloud and replace its neighbor points into the first point cloud. As the new sample obtained by the second replacement method in Euclidean space conserves the semantic relations among its neighbors, so it has better effect than random replacement [21]. However, every point in the manifold is far away from other points. Therefore, the nearest neighbor replacement loses its advantage in this scenario, and the effect of random replacement is better, which is supported in the experiment section.

**T-net after PointManifoldCut.** T-net [22] is a mini-network that learns affine transformation matrix and usually takes the original point clouds as input [7, 9] to ensure the model's invariance to spatial transformation. We always set the T-net after PointManifoldCut operation instead of immediately after input to unify the transformation invariance of new samples in manifold, which can be described as:

$$t(g_k(\tilde{p})) = A \times g_k(\tilde{p}), A \in \mathbb{R}^d \times \mathbb{R}^d \quad (5)$$

where  $t$  and  $A$  respectively denotes the spatial transform operation and the transformation matrix output by T-net.  $d$  is the feature dimension of layer  $k$ . In PointNet, a regularization term is set to restrict the transformation matrix to a form that is close to the orthogonal matrix, thus reducing the difficulty of optimization. This is also be used in our work, as described as:

$$L_{reg} = \|I - AA^T\|^2 \quad (6)$$

where  $L_{reg}$  represent the regularization term added to the training loss and  $I$  is an identity matrix of the same size as transformation matrix  $A$ .

### 3 Experiments

#### 3.1 Experiments Setup

**Datasets.** We use two point cloud datasets in our experiments. ModelNet40 [15] contains 12311 CAD samples from 40 object categories, while each sample consists of 2048 points. Among them, 9843 models are used for training and the other 2468 models are left out as the test set. ShapeNet [16] parts contains 16880 samples from 16 categories and 50 part labels, it is split into 14006 for training and 2874 for testing. Both datasets are publicly available, and we use the ModelNet40 for the point cloud classification experiments while run point cloud segmentation experiments on the ShapeNet dataset.

**Networks.** To show that PointManifoldCut is a general technique and agnostic to the network which is employed, we experiment with three cutting edge network architectures, including PointNet [7], PointNet++ [8], and DGCNN [9], where PointNet learns the features based solely on one point and does not consider the neighbor information, PointNet++ obtains multi-level local features by hierarchical sampling, and DGCNN builds dynamic local graphs at each layer based on the k-nearest neighbors method.

**Implementation details.** We implement our work in PyTorch [23]. All the networks used in the experiments take 2048 points as an input point cloud instance. Each experiment runs for 250 epoches with a batch size of 16 on a NVIDIA Quadro RTX 5000 GPU card. We use the Adam [24] optimizer with an initial learning rate of 0.001 that decays by half every 20 epoches to train the PointNet and PointNet++. DGCNN is trained with the SGD [25] optimizer with an initial learning rate of 0.1, which is reduced until 0.001 through cosine annealing. The momentum for batch normalization of SGD is 0.9 and the batch normalization decay is not used.

Method	PointNet	PointNet++	DGCNN
Baseline	89.2	90.7	92.3
PointMixup	89.9	92.7	93.1
PointCutMix	89.9	<b>93.4</b>	93.2
PointManifoldCut-K	89.4	92.9	93.1
PointManifoldCut-R	<b>90.0</b>	93.0	<b>93.7</b>

Table 1: **Performance with different augmentations on Modelnet40.** Metric is overall accuracy(%).

#### 3.2 Classification

We perform experiments on ModelNet40 dataset to show how PointManifoldCut improves the performance in object-level task with respect to the different locations in the network where PointManifoldCut is applied to.

**Comparison to other point cloud augmentation methods.** Here, we compare the improvements brought by PointManifoldCut and other point cloud augmentation technologies, including PointMixup [20] and PointCutMix [21], on several classification networks. From Table 1, it can be seen that PointManifoldCut improves the classification performance of DGCNN most significantly, about 1.4%, 0.6% and 0.5% higher than PointMixup and PointCutMix. For PointNet, the three augmentations show similar improvement over the vanilla model. When the baseline network is PointNet++, the effect of PointManifoldCut is between PointMixup and PointCutMix, 0.3% higher than the former and 0.4% lower than the latter. In general, our PointManifoldCut improves the overall accuracy of cutting-edge point cloud classification networks by 0.8% to 2.3%, which is competitive compared with the existing methods.

**The layer  $k$  where PointManifoldCut is applied to.** We further investigate the impact of site where PointManifoldCut is inserted into the DGCNN on the model performance. DGCNN dynamically constructs local graphs and learns features through four consecutive EdgeConv [9] layers. Fig. 3 shows the overall accuracy and mean-class accuracy of using PointManifoldCut after these four different EdgeConv layers. It can be seen that the effect is similar for each case. But when PointManifoldCut is applied to latter layer (layer-3), the overall accuracy and mean class accuracy are higher than the second performance by 0.6% and 0.5% respectively.

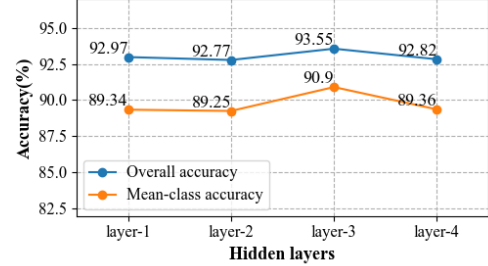


Figure 3: **Performance comparison when PointManifoldCut is applied to layer  $k$ .**  $\rho = 1$  and  $\beta = 0.5$  are used in this experiment.

Besides, we compare the two replacement schemes of points introduced in Sec. 2.3, where PointManifoldCut-K and PointManifoldCut-R represent the nearest neighbor replacement and random replacement used respectively. It is shown that random replacement is generally better than nearest neighbor replacement in the manifold.

#### 3.3 Part segmentation

Point cloud segmentation is another important task in point cloud learning. We discuss the impact of point-wise features at different levels on PointManifoldCut, and then compare its performance improvement with existing method on ShapeNet parts dataset. Since PointMixup lacks interpolated point labels, the comparison here focuses on

Method	mIoU	Air plane	Bag	Cap	Car	Chair	Ear phone	Gui- tar	Knife	Lamp	Lap- top	Motor bike	Mug	Pistol	Roc- ket	Skate board	Table
		2690	76	55	898	3758	69	787	392	1547	451	202	184	283	66	152	5271
PointNet	83.1	82.2	72.3	79.1	72.0	89.2	72.9	90.0	84.8	78.2	95.0	62.3	89.9	81.2	52.4	73.1	81.9
+PCM	83.7	82.0	70.6	77.6	75.1	89.6	<b>73.9</b>	90.3	85.9	78.8	95.1	63.8	<b>91.8</b>	80.3	53.7	72.7	82.4
+Ours	<b>84.2</b>	<b>83.2</b>	<b>76.7</b>	<b>80.7</b>	<b>75.9</b>	<b>90.0</b>	72.5	<b>90.2</b>	<b>86.0</b>	<b>79.6</b>	<b>95.3</b>	<b>66.3</b>	91.1	<b>82.2</b>	<b>55.5</b>	<b>73.3</b>	<b>82.8</b>
PointNet2	84.9	82.1	83.0	82.3	77.4	90.2	69.9	90.8	86.9	84.3	95.2	68.6	94.1	82.7	60.2	74.4	82.8
+PCM	<b>85.5</b>	82.6	<b>85.9</b>	83.7	<b>78.3</b>	90.7	72.5	90.9	<b>87.7</b>	84.3	<b>95.3</b>	<b>70.7</b>	<b>95.1</b>	82.4	<b>62.3</b>	<b>74.9</b>	<b>83.4</b>
+Ours	85.3	<b>82.6</b>	85.2	<b>84.9</b>	78.1	<b>90.9</b>	<b>73.3</b>	<b>91.3</b>	87.1	<b>84.4</b>	95.2	69.9	94.4	<b>82.9</b>	58.6	74.5	82.6
DGCNN	85.2	84.0	83.4	86.7	77.8	90.6	74.7	91.2	87.5	82.8	95.7	66.3	<b>94.9</b>	81.1	<b>63.5</b>	74.5	82.6
+PCM	85.7	84.1	<b>84.5</b>	87.6	<b>78.1</b>	91.0	<b>77.7</b>	91.6	<b>88.9</b>	84.4	95.9	68.9	94.6	<b>83.1</b>	60.3	<b>75.6</b>	<b>83.0</b>
+Ours	<b>85.7</b>	<b>84.2</b>	83.3	<b>87.8</b>	77.6	<b>91.1</b>	73.3	<b>91.6</b>	88.7	<b>84.7</b>	<b>96.0</b>	<b>71.5</b>	94.4	82.4	59.8	73.8	82.9

Table 2: **Improvements of segmentation with different augmentations on ShapeNet part dataset.** The Metric is mIoU(%) on points. PCM indicates the PointCutMix augmentation method. The first row is the sample size of the corresponding category.

PointCutMix. We choose mIoU(mean Intersection-over-Union) as the evaluation metric of point cloud segmentation task, which is calculated by averaging the IoUs of all the testing shapes.

Layers	PointNet		DGCNN	
	After-T	Before-T	After-T	Before-T
Layer-1	83.40	84.25	85.52	85.71
Layer-2	83.52	83.63	85.30	85.44
Layer-3	83.31	83.70	85.51	85.53
Baseline	83.13		85.23	

Table 3: **mIoU when PointManifoldCut applied on different hidden layers.** The After-T column lists the value when PointManifoldCut is applied after T-net; The Before-T column shows the value when PointManifoldCut is applied before T-net.

**Comparison to other augmentation.** Here, we show in detail the improvement effect of PointManifoldCut on the point-wise classification task of three deep networks, including PointNet, PointNet++ and DGCNN, as well as the comparison with PointCutMix. From Table 2, a notable improvement of PointManifoldCut on the segmentation metrics of PointNet can be seen, with a total increase of 1.1%, which is 0.5% higher than that of PointCutMix. Since PointNet hardly capture the local information, this promotion does not come from the smooth combination of samples, but because the combination of samples in the manifold domain are more meaningful. However, PointManifoldCut has limited improvement on PointNet++ and lags behind PointCutMix by 0.3%. It may because that we only replace points after feature inverse interpolation, resulting in insufficient learning of new samples. For DGCNN, PointManifoldCut and PointCutMix both improve the performance of segmentation by about 0.5%.

**The layer  $k$  where PointManifoldCut is applied to.** We firstly compare the influences of replacing different levels

of point-wise features on point cloud segmentation tasks. DGCNN uses three EdgeConv layers to capture local features in segmenting branch, while PointNet also sets up a three-layer perceptron before concatenating the category vector. So we use PointManifoldCut in the first three hidden layers to see if there is a significant impact. At the same time, we compare the effect of setting the spatial transform before or after using PointManifoldCut operation. Because the sampling layers of PointNet++ continuously reduces the scale of point set, PointManifoldCut for PointNet++ is only used after all points get high-dimensional features through inverse interpolation.

As shown in Table 3, different-level hidden representation has greater influence on segmentation task than that of classification task, which may be that segmentation task is more sensitive to point-wise features. We also observed a similar trend in the improvement effect of PointManifoldCut on PointNet and DGCNN, which is the most significant in layer-1, then decreased in layer-2 and rebounded in layer-3. This may indicate that the features of the first hidden layer represent the most meaningful new samples constructed. And setting spatial transform after PointManifoldCut is better than before.

### 3.4 Robustness test

In addition to the direct improvement of our augmentation method on the performance of deep neural network in point cloud classification and segmentation tasks, we further discuss its impact on the robustness of these networks. We focus on two common point cloud attacks: point dropping and adding random noise. Point dropping [26] refers to the random dropping of a portion of points in a point cloud random, and PointDrop(0.2) means the dropped points account for one fifth of the total points. Similar to image domain, gaussian noise with different variance is randomly added to the three coordinates of points to attack the networks. We apply these two attacks on the test set, and then report the performance of the networks trained with the normal training set. Below are the results.

**Point cloud classification.** We conducted six attacks on the test set of ModelNet40 in Table 4, and then show the classification accuracy of DGCNN with and without PointManifoldCut training. It can be seen that PointManifoldCut brings remarkable additional robustness to DGCNN, and it becomes more obvious as the attack intensifies. When randomly dropping one tenth of points, PointManifoldCut only improves the overall accuracy of 1.4% and the mean-class accuracy of 0.6%. However, when the dropping ratio increased to 0.3, the two indicators increased by 4.1% and 2.5% respectively. Compared to point dropping, our augmentation method has better stability when adding noise. In the face of gaussian noise with variance of 0.001, PointManifoldCut can improve the overall accuracy as well as mean-class accuracy by nearly 10%. When the variance increases to 0.003, the overall accuracy of the original DGCNN decreases to 33.5%, but it can be stabilized at about 53.0% after using PointManifoldCut, and the increment is about 19.5%.

Attack	DGCNN+ PointManifoldCut			
	OA(%)	MA(%)	OA(%)	MA(%)
PointDrop(0.1)	82.76	80.90	84.15	81.46
PointDrop(0.2)	75.20	73.15	75.90	73.50
PointDrop(0.3)	64.30	63.04	68.38	65.56
Noise var=0.001	72.18	62.56	82.03	72.31
Noise var=0.002	49.59	41.26	66.05	54.09
Noise var=0.003	33.50	27.71	52.98	42.76

Table 4: **Robustness test on ModelNet40.** Var is the variance of the added gaussian noise.

**Point cloud segmentation.** Then we evaluate the impact of PointManifoldCut on the robustness of segmentation tasks. Since points dropping will hinder the calculation of mIoU, we focus on adding gaussian noise here. From Table 5, we first note that the original PointNet is more robust than DGCNN, because the latter will be subject to additional damage caused by local feature contamination. PointNet does not consider the neighborhood information, resulting in stronger stability. Similar to the classification task, PointManifoldCut also brings remarkable robustness improvement in segmentation.

Variance	PointNet		DGCNN	
	Baseline	+PMC	Baseline	+PMC
Clean	83.13	84.25	85.23	85.71
0.001	77.55	79.18	76.48	79.78
0.002	73.91	75.88	72.11	75.93
0.003	70.84	72.85	68.41	72.65

Table 5: **mIoU of networks under different variance noise.** The clean row lists the result when no noise is added.

For PointNet, the performance of PointManifoldCut in three gaussian noise intensities is around 2% higher than that of the original network. Moreover, this improvement will slowly increase with the enhancement of noise. When

the variance is 0.001, PointManifoldCut brings an additional 3.3% improvement for DGCNN. However, when the variance increases to 0.003, the mIoU of the baseline is 68.4%, which increases to 72.7% after using PointManifoldCut, with an difference of 4.3%.

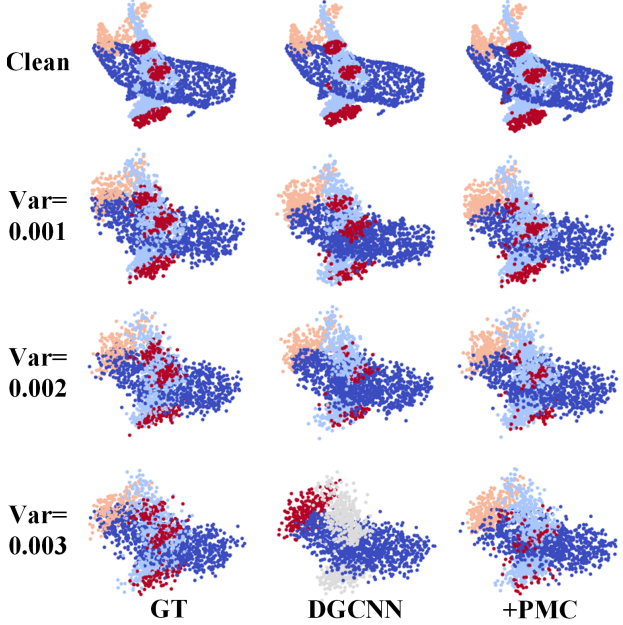


Figure 4: **Segmentation results of DGCNN on ShapeNet part dataset.** Each row represents the input with different variance gaussian noise. The first column is the ground truth, the second column is the output of the original DGCNN, while the third column is the output with PointManifoldCut. The color illustrates the category of the part to which the point belongs.

Fig. 4 shows the visual segmentation results of DGCNN before and after using PointManifoldCut under gaussian noise with different intensity. It can be clearly seen that although the part segmentation effect of DGCNN on the aircraft model is close to the ground truth without gaussian noise, there are still some bad judgments. When the variance increases to 0.003, the segmentation ability of DGCNN decreases rapidly. It identifies all wings and engines as other categories, and almost all tails as engines. However, after using PointManifoldCut, the fuselage, wing, tail and engine are identified and roughly matched.

## 4 Conclusion

We presented PointManifoldCut point-wise augmentation method for point cloud, which explores the points mix-up options and the possible site that the method is applied. The experiments suggest that our method outperforms other point augmentation methods on cutting-edge point cloud neural networks. However, A future research direction is to embed the structural information of the point clouds during the data augmentation to further regularize the point cloud learning models.

## References

- [1] Ji Zhang and Sanjiv Singh. Low-drift and real-time lidar odometry and mapping. *Autonomous Robots*, 41:401–416, 2017.
- [2] Miao Liao, Feixiang Lu, Dingfu Zhou, Sibo Zhang, Wei Li, and Ruigang Yang. Dvi: Depth guided video inpainting for autonomous driving. In *ECCV*, 2020.
- [3] J. Wijesingha, Thomas Möckel, F. Hensgen, and M. Wachendorf. Evaluation of 3d point cloud-based models for the prediction of grassland biomass. *Int. J. Appl. Earth Obs. Geoinformation*, 78:352–359, 2019.
- [4] Yuxing Xie, Jiaoqiao Tian, and X. X. Zhu. Linking points with labels in 3d: A review of point cloud semantic segmentation. *IEEE Geoscience and Remote Sensing Magazine*, 8:38–59, 2020.
- [5] Yulan Guo, Hanyun Wang, Qingyong Hu, Hao Liu, Li Liu, and M. Bennamoun. Deep learning for 3d point clouds: A survey. *IEEE transactions on pattern analysis and machine intelligence*, PP, 2020.
- [6] Min Zhang, Haoxuan You, Pranav Kadam, Shan Liu, and C.-C. Jay Kuo. Pointhop: An explainable machine learning method for point cloud classification. *IEEE Transactions on Multimedia*, 22:1744–1755, 2020.
- [7] C. Qi, Hao Su, Kaichun Mo, and L. Guibas. Pointnet: Deep learning on point sets for 3d classification and segmentation. In *CVPR*, 2017.
- [8] C. Qi, L. Yi, Hao Su, and L. Guibas. Pointnet++: Deep hierarchical feature learning on point sets in a metric space. In *NIPS*, 2017.
- [9] Yue Wang, Yongbin Sun, Ziwei Liu, Sanjay E. Sarma, M. Bronstein, and J. Solomon. Dynamic graph cnn for learning on point clouds. *ACM Transactions on Graphics*, 38:1 – 12, 2019.
- [10] Florent Poux and R. Billen. Voxel-based 3d point cloud semantic segmentation: Unsupervised geometric and relationship featuring vs deep learning methods. *ISPRS Int. J. Geo Inf.*, 8:213, 2019.
- [11] Chenfeng Xu, B. Wu, Zining Wang, W. Zhan, Péter Vajda, K. Keutzer, and M. Tomizuka. Squeezesegv3: Spatially-adaptive convolution for efficient point-cloud segmentation. In *ECCV*, 2020.
- [12] Mingye Xu, Zhipeng Zhou, and Y. Qiao. Geometry sharing network for 3d point cloud classification and segmentation. *ArXiv*, abs/1912.10644, 2020.
- [13] Chen-Hsuan Lin, Chen Kong, and S. Lucey. Learning efficient point cloud generation for dense 3d object reconstruction. In *AAAI*, 2018.
- [14] Xiangyu Yue, B. Wu, S. Seshia, K. Keutzer, and A. Sangiovanni-Vincentelli. A lidar point cloud generator: from a virtual world to autonomous driving. *Proceedings of the 2018 ACM on International Conference on Multimedia Retrieval*, 2018.
- [15] Zhirong Wu, Shuran Song, A. Khosla, F. Yu, Linguang Zhang, Xiaou Tang, and J. Xiao. 3d shapenets: A deep representation for volumetric shapes. In *CVPR*, pages 1912–1920, 2015.
- [16] Angel X. Chang, T. Funkhouser, L. Guibas, P. Hanrahan, Qixing Huang, Zimo Li, S. Savarese, M. Savva, Shuran Song, Hao Su, J. Xiao, L. Yi, and F. Yu. Shapenet: An information-rich 3d model repository. *ArXiv*, abs/1512.03012, 2015.
- [17] Hongyi Zhang, Moustapha Cissé, Yann Dauphin, and David Lopez-Paz. mixup: Beyond empirical risk minimization. *ArXiv*, abs/1710.09412, 2018.
- [18] Vikas Verma, Alex Lamb, Christopher Beckham, Amir Najafi, Ioannis Mitliagkas, David Lopez-Paz, and Yoshua Bengio. Manifold mixup: Better representations by interpolating hidden states. In *ICML*, 2019.
- [19] Sangdoo Yun, Dongyoon Han, Seong Joon Oh, Sanghyuk Chun, Junsuk Choe, and Y. Yoo. Cutmix: Regularization strategy to train strong classifiers with localizable features. In *ICML*, pages 6022–6031, 2019.
- [20] Yunlu Chen, Vincent Tao Hu, E. Gavves, Thomas Mensink, P. Mettes, Pengwan Yang, and Cees Snoek. Pointmixup: Augmentation for point clouds. In *ECCV*, 2020.
- [21] Jinlai Zhang, Lvjie Chen, Bojun Ouyang, Binbin Liu, Jihong Zhu, Yujing Chen, Yanmei Meng, and Danfeng Wu. Pointcutmix: Regularization strategy for point cloud classification. *ArXiv*, abs/2101.01461, 2021.
- [22] Max Jaderberg, K. Simonyan, Andrew Zisserman, and K. Kavukcuoglu. Spatial transformer networks. In *NIPS*, 2015.

- [23] Adam Paszke, S. Gross, Francisco Massa, Adam Lerer, James Bradbury, Gregory Chanan, Trevor Killeen, Zeming Lin, N. Gimelshein, L. Antiga, Alban Desmaison, Andreas Köpf, E. Yang, Zach DeVito, Martin Raison, Alykhan Tejani, Sasank Chilamkurthy, Benoit Steiner, Lu Fang, Junjie Bai, and Soumith Chintala. Pytorch: An imperative style, high-performance deep learning library. In *NeurIPS*, 2019.
- [24] Diederik P. Kingma and Jimmy Ba. Adam: A method for stochastic optimization. *CoRR*, abs/1412.6980, 2015.
- [25] Priya Goyal, Piotr Dollár, Ross B. Girshick, P. Noordhuis, Lukasz Wesolowski, Aapo Kyrola, Andrew Tulloch, Y. Jia, and Kaiming He. Accurate, large minibatch sgd: Training imagenet in 1 hour. *ArXiv*, abs/1706.02677, 2017.
- [26] Tianhang Zheng, Changyou Chen, Junsong Yuan, B. Li, and Kui Ren. Pointcloud saliency maps. In *NIPS*, pages 1598–1606, 2019.